Asian Journal of Pharmaceutical Sciences 17 (2022) 435–446

Available online at www.sciencedirect.com

ScienceDirect

journal homepage: www.elsevier.com/locate/AJPS

Original Research Paper

New modular platform based on multi-adjuvanted amphiphilic chitosan nanoparticles for efficient lipopeptide vaccine delivery against group A streptococcus

Abdin Shakirin Mohamad Norpi[a,b], *Muhammad Luqman Nordin*[a,c], *Nuraziemah Ahmad*[a], *Haliza Katas*[a], *Abdullah Al-Hadi Ahmad Fuaad*[d], *Asif Sukri*[e], *Nirmal Marasini*[f], *Fazren Azmi*[a,*]

[a] *Centre for Drug Delivery Technology, Faculty of Pharmacy, Universiti Kebangsaan Malaysia, Kuala Lumpur 50300, Malaysia*
[b] *Faculty Pharmacy and Health Sciences, Universiti Kuala Lumpur, Royal College of Medicine Perak, Perak 30450, Malaysia*
[c] *Faculty of Veterinary Medicine, Universiti Malaysia Kelantan, Kelantan 16100, Malaysia*
[d] *Department of Chemistry, Faculty of Science, Universiti Malaya, Kuala Lumpur 50603, Malaysia*
[e] *Universiti Teknologi Mara (UiTM), Bandar Puncak Alam, Integrative Pharmacogenomics Institute (iPROMISE), Selangor 43200, Malaysia*
[f] *School of Biomedical Sciences, The University of Queensland, St. Lucia QLD 4072, Australia*

ARTICLE INFO

Article history:
Received 17 June 2021
Revised 1 April 2022
Accepted 6 April 2022
Available online 30 April 2022

Keywords:
Amphiphilic chitosan nanoparticles
Peptide vaccine
Lipidation
Multi-adjuvanting delivery system
Immunogenicity
Group A streptococcus

ABSTRACT

An effective vaccine against group A streptococcus (GAS) is highly desirable for definitive control of GAS infections. In the present study, two variants of amphiphilic chitosan nanoparticles-based GAS vaccines were developed. The vaccines were primarily composed of encapsulated KLH protein (a source of T helper cell epitopes) and lipidated M-protein derived B cell peptide epitope (lipoJ14) within the amphiphilic structure of nanoparticles. The only difference between them was one of the nanoparticles vaccines received additional surface coating with poly (I:C). The formulated vaccines exhibited nanosized particles within the range of 220–240 nm. Cellular uptake study showed that nanoparticles vaccine without additional poly (I:C) coating has greater uptake by dendritic cells and macrophages compared to nanoparticles vaccine that was functionalized with poly (I:C). Both vaccines were found to be safe in mice and showed negligible cytotoxicity against HEK293 cells. Upon immunization in mice, both nanoparticle vaccines produced high antigen-specific antibodies titres that were regulated by a balanced Th1 and Th2 response compared to physical mixture. These antibodies elicited high opsonic activity against the tested GAS strains. Overall, our data demonstrated that amphiphilic chitosan nanoparticles platform induced a potent immune response even without additional inclusion of poly (I:C).

* Corresponding author.
E-mail address: fazren.azmi@ukm.edu.my (F. Azmi).
Peer review under responsibility of Shenyang Pharmaceutical University.

https://doi.org/10.1016/j.ajps.2022.04.002

1. Introduction

Group A Streptococcus (GAS) is listed among the top ten pathogens that responsible for high rates of mortality and morbidity on a global scale. World Health Organization (WHO) estimates that more than 100 million people worldwide suffered from GAS-related diseases and half a million deaths were reported each year [1,2]. Infections caused by GAS are responsible for a vast array of diseases from relatively mild illnesses, such as pharyngitis and impetigo, to invasive infections (e.g., cellulitis and necrotizing pharyngitis). The autoimmune sequelae of GAS infections can also lead to acute rheumatic fever and chronic rheumatic heart disease, which can be fatal [3]. Unnecessary use of antibiotics for GAS infections has also exacerbated the spread of antimicrobial resistance [4,5]. Thus, an effective vaccine is highly needed as a preventive strategy for various GAS infections and their immune-driven complications.

Currently, there is still no licensed vaccine available against GAS despite decades of research [5]. A vast number of researches have been focusing on the development of M-protein based GAS vaccines [6]. M protein is regarded as the primary virulence factor of GAS. However, antibodies against M protein have high propensity to cross-react with human cardiac tissue, thus limiting its application for clinical use [7–9]. This situation has also made the conventional vaccine approaches, like using the killed or attenuated form of whole GAS as antigen, not feasible [9].

Alternatively, the use of peptide-based vaccine offers substantial advantages in terms of safety profiles in developing a GAS vaccine. This form of vaccine contains only essential antigenic determinant(s) of the protein epitopes, thus allowing the induction of highly selective immune responses. A chimeric peptide, termed J14 (KQAEDKVK**ASREAKKQVEKALE**QLEDKVK), which contain minimal B cell epitope (amino acids highlighted in bold) derived from the conserved region of M protein flanked with α-helix-inducing sequences (to recapitulate the native M-protein structure) was identified as a promising vaccine candidate against GAS [10]. However, synthetic peptide vaccines, such as J14 is insufficient to elicit immune response on their own. Thus, peptide vaccines need to be administered alongside adjuvants, not only to confer protection, but also to mediate their recognition by immune cells for further processing by immune cells. Various adjuvanting strategies have emerged to improve peptides immunogenicity, including their conjugation to a carrier protein, co-administration with toll-like receptor (TLR) agonist(s), encapsulation in nanoparticles, or a combination of several approaches [11–13].

Nanoparticles are known to exhibit structural similarities to the virus due to their nanoscale dimension and multivalent antigen presentation for efficient immune cells recognition. Nanoparticles composed of chitosan confer several advantages for vaccine delivery, such as being biodegradable, biocompatible, nontoxic, possess immunostimulatory properties and contain reactive functional groups for chemical modification [14,15]. In this study, we have chemically functionalized chitosan with arginine and oleic acid through its reactive amino groups, dubbed as amphiphilic chitosan nanoparticles (ACNs), to improve its chemical and adjuvanting properties. Oleic acid possesses intrinsic immunostimulant properties while the arginine-functionalized chitosan may not only improve its water solubility, but also intensified the positive charges on chitosan molecule for efficient uptake by antigen-presenting cells (APCs) [16,17].

Peptide lipidation is an established strategy to enhance the peptide's stability and immunogenicity effect. This strategy conceptualized the idea of mimicking a lipoprotein structure of bacteria, that is commonly recognized by innate immune cells [16]. Various types of lipid moieties, such as Pam2Cys, Pam3Cys and lipoaminoacids when covalently linked to peptide epitopes induced an enhanced immune response [18–20]. Inspired by this outcome, we have conjugated two copies of palmitic acid (C16) to J14 by using additional lysine residue as a branching core (Fig. 1). We also sought that this lipidation strategy would enhance the peptide encapsulation efficiency within the ACNs due to the greater hydrophobic interaction.

A series of GAS vaccine formulations with systematic composition variations were formulated to investigate the role of immunostimulating components in influencing the magnitude of antibodies production against J14 (Fig. 1). The vaccine formulations were composed of our novel ACNs as the nanoparticle's core, lipidated J14 (lipoJ14) intercalated within the lipidic portion of ACNs, keyhole limpet hemocyanin (KLH) and the formulation with/without additional coating with polyinosinic-polycytidylic acid, poly(I:C) - a ligand of TLR 3. In contrast to the conventional KLH-hapten conjugation strategy, the KLH was encapsulated at the ACNs core to serve as the source of T helper epitopes, instead of a carrier protein. This strategy envisaged to minimize the possibility of antibodies elicitation against KLH. Our overall peptide GAS vaccine formulation strategy conferred the advantages of concomitant delivery of vaccine antigen and immunopotentiators in single nanoparticulate platform for efficient presentation to immune cells.

The physicochemical properties of the nanoparticle vaccine formulations were characterized for their particle size, morphology, and size distribution (given as polydispersity index). The uptake efficiency of the nanoparticles by professional APCs, particularly dendritic cells (DCs) and macrophages were investigated. The immunogenicity of the vaccine constructs was evaluated in mice. An additional vaccine formulation based on physical mixtures of lipoJ14, ACNs and KLH was also assessed to elucidate the role of nanoparticle architecture in mediating immune cells activation. The spectrum of cytokines responses was quantified following mice immunization. Finally, the obtained sera from vaccinated mice were assessed for their capacity in generating opsonisation effects against various GAS strains. The toxicity effects of the vaccines were examined using both *in vitro* and *in vivo* model.

2. Materials and methods

2.1. Materials

Keyhole lymphocyiate haemocyanin (KLH), chitosan (low molecular weight, 85% deacetylated), L-arginine, oleic acid,

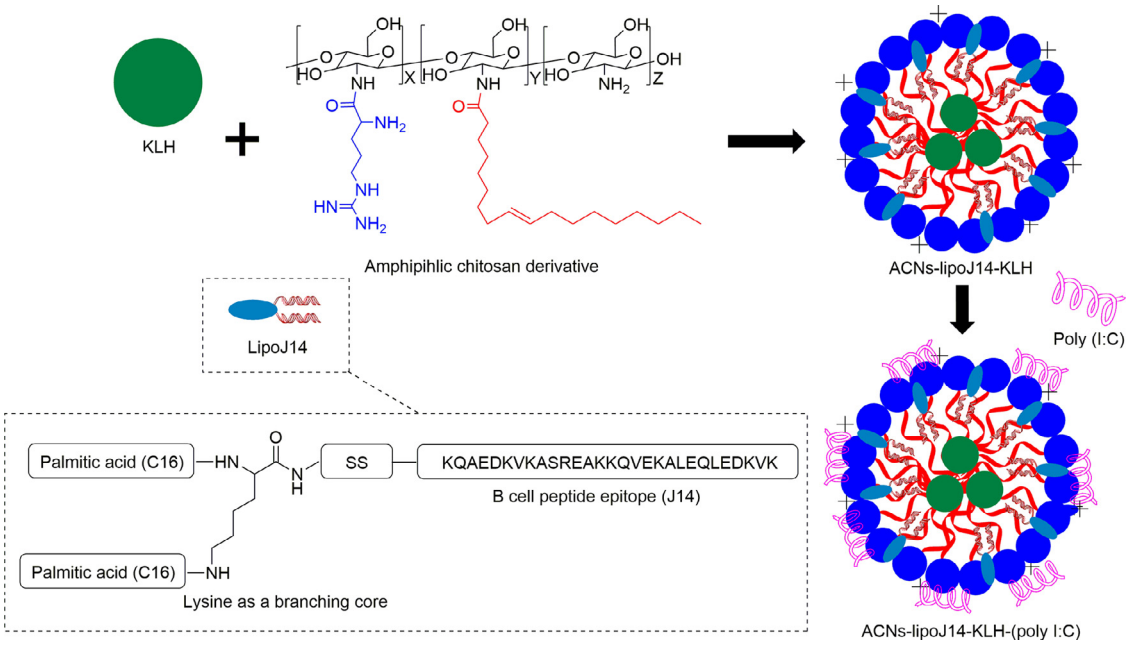

Fig. 1 – Schematic presentation of the developed nanoparticles GAS vaccine formulations and the structure of chemically synthesized lipoJ14.

glacial acetic acid, low molecular weight polyinosinic-polycytidylic acid (poly (I:C)), benzoylated dialysis tubing (MWCO 2000), MES buffer and lysis buffer were purchased from Sigma-Aldrich (USA). N-(−3-dimethylaminopropyl)-N-ethylcarbodiimide hydrochloride (EDC) was purchased from Santa Cruz Biotechnology, Inc (USA). *N*,*N*-Dimethyl-formamide (DMF) was purchased from Merck (Germany). Eagle's Minimum Essential Medium (EMEM) was supplied by Addexbio (USA). IMDM Glutamax medium Fetal Bovine Serum (FBS), Gibco^{TM} Penicillin-Streptomycin liquid and 2-mercaptoethanol (50 µM) were obtained from Thermo Fisher Scientific (USA). CD11c was obtained from eBioscience (USA) while F4/80 was purchased from BioLegend, Pacific, (USA). Antimouse IgG, IgG1 and IgG2a conjugated to horseradish peroxidase were purchased from Sigma-Aldrich (USA). All the chemicals and reagents were of analytical grade and required no further purification before use.

The lipoJ14 (C16-K(C16)SSKQAEDKVKASREAKKQVEKAL-EQLEDKVK) and J14 (KQAEDKVKASREAKKQVEKALEQLEDKVK) were synthesized by Bankpeptide Co., Ltd. (Hefei, China). The theoretical mass of the lipoJ14 was 4132.98 Da and the calculated parent ion was 4133.80 Da as determined by ESI-MS. For J14 (KQAEDKVKASREAKKQVEKALEQLEDKVK), the theoretical mass was 3354.81 Da while the observed parent ion by ESI-MS was 3355.05 Da. Peptides were obtained as white to off-white lyophilized powder with a purity of more than 95% as analysed by analytical RP-HPLC.

2.2. *Synthesis of amphiphilic chitosan derivative*

The amphiphilic chitosan derivative was prepared by conjugating arginine and oleic acid to the free amino groups present in the chitosan backbone via carbodiimide chemistry according to our established protocol [21]. Briefly, 1.5 ml 1% (v/v) oleic acid/DMF was added to 2% (w/v) EDC in sodium acetate buffer at pH 6.4. Chitosan (1 mg/ml) was dissolved in a 0.1 M sodium acetate buffer solution. The solution mixture containing oleic acid and EDC was added dropwise into the chitosan solution to a total volume of 20 ml at pH 6.4 under continuous magnetic stirring at room temperature for 24 h. Next, 1 mg/ml of arginine was dissolved in 0.1 M sodium acetate buffer at pH 6.4 followed by a drop-wise addition of 2% (w/v) EDC in sodium acetate buffer (pH 6.4) solution. The reaction mixture of arginine and EDC solution was slowly added into the mixture of chitosan-oleic acid under continuous magnetic stirring at room temperature for 24 h. The resultant suspension of chitosan coupled with arginine and oleic acid (amphiphilic chitosan derivative) was purified by using MWCO 2000 benzoylated dialysis tubing in distilled water for another 24 h. The weight ratio of chitosan to oleic acid and arginine used was (1:5:1). The purified solutions were lyophilized and stored at −20 °C until further use. The FTIR spectra of chitosan and the newly synthesized amphiphilic chitosan derivative were recorded using a Spectrum 100 Fourier Transform Infrared Spectroscopy (Perkin Elmer, USA) with an average of 40 scans at a resolution of 4 cm^{-1}, at a wavelength range within 650 to 4000 cm^{-1}. Next, the lyophilized amphiphilic chitosan compound was dissolved in deuterated chloroform to determine the conjugation chitosan with (oleic acid and arginine) by using ^{1}HNMR.

2.3. *Nanoparticles vaccine formulations*

The ACNs were prepared through ionic gelation method. Firstly, the synthesized amphiphilic chitosan derivative was dissolved in 0.5% (v/v) in acetic acid to make a 1 mg/ml

solution. Then, 300 ug peptide (lipoJ14) was dissolved in deionized water and incubated together with the amphiphilic chitosan solution. Then, a 150 µg KLH and 10 µl 0.25 mg/ml of TPP were added to the chitosan mixture and stirred continuously for 1 h at room temperature. The TPP concentration was selected based on optimization of the zeta potential and size uniformity of ACNs (Table S1, supplementary material). The ACNs coated with poly (I:C) was prepared by adding a 75 µl 1 mg/ml poly (I:C) dropwise into a 0.9 ml ACNs solution (1 mg/ml) under continuous stirrer for 1 h at room temperature. The optimum amount of poly (I:C) required to coat the surface of ACNs was selected based on charge reversal, particle size and polydispersity index (PDI) (Table S2, supplementary material).

2.4. Encapsulation efficiency

The content of lipoJ14 in the nanoparticles was determined by using standard calibration curve based on known concentration of lipoJ14. The ACNs formulation was centrifuged using Beckman Coulter Optima L-100 XP Floor Ultracentrifuge System at 30 000 rpm for 1 h at 4 °C. The absorption of free lipoJ14 in the supernatants was read by using UV spectrophotometer at 202 nm and calculated by using the following formula. Similar method was used to obtain encapsulation efficiency of KLH (UV detectionat a wavelength 232 nm) in the nanoparticles.

$$\text{EE (\%)} = \frac{\text{Total lipoJ14(ug)} - \text{Amount of free lipoJ14(ug)}}{\text{lipoJ14 (ug)}} \times 100\%$$

2.5. Nanoparticles characterizations

Particle size, PDI value and zeta potential of the formulated nanoparticle vaccines were measured using Malvern Zetasizer Nano ZS (UK). The measurements were performed at 25 °C using disposable folded capillary cells, in triplicate. Samples were dispensed in distilled water before measurement. The morphology of the nanoparticles was examined by using Talos L120C (Thermo Fisher, USA) transmission electron microscope (TEM) at an accelerating voltage of 100 kV. A drop of samples (at 10 × dilution) was placed to a carbon-coated 200 mesh grid and left for air-dried at room temperature for 5 min, before viewing by TEM.

2.6. Uptake of vaccine constructs by dendritic cells (DC) and macrophages in in vitro model

Uptake assay of the formulated nanoparticle vaccines was performed based on an established protocol with slight modification [22]. In brief, the nanoparticle vaccines were initially labelled with Dil (1,1 dioctadecyl-3,3,30,30 tetramethylindocarbocyanine perchlorate). The CD11c and F4/80 antibodies were used to identify the DCs and macrophages, respectively. The mice spleens were harvested and homogenized by passing through a cell strainer to obtain single cell suspension, and erythrocytes were lysed by using erylysis buffer (pH 7.2–7.4, sterilized). Then, the resultant splenocytes were seeded into a 12-well plate (at a cell density of 2×10^5 cells/well) in a phenol-free IMDM Glutamax medium, supplemented with 10% FBS, 50 µM 2-mercaptoethanol, 100 IU/ml penicillin, and 100 µg/ml streptomycin. Vaccine candidates labelled with Dil were added to the wells and incubated overnight. The adherent cells were scraped from the plate and incubated with Fc-block for 20 min at 4 °C, centrifuged and resuspended in a buffer containing CD11c and F4/80 antibodies for 30 min at 4 °C. The cells were then centrifuged and resuspended in 0.5 ml of FACS buffer (PBS, 0.02% sodium azide, 0.5% BSA). The uptake of the nanoparticle vaccines by DCs and macrophages was quantified using LSR II flowcytometer (BD FacsCanto II, CA, USA). The fluorescence intensities of dendritic cells and macrophages treated with normal saline were also measured as a control. The actual uptake was calculated as the percentage of cells for Dil and CD11c or Dil and F4/80.

2.7. Mice immunization

The study's protocol was approved by Universiti Kebangsaan Malaysia (UKM) Animal Ethics Committee (UKMAEC) with approval code: FF/2019/FAZREN/24-JULY/1025-AUG-2019-AUG 2020. Six-week-old female Balb/c mice obtained from the UKM Laboratory Animal Research Unit (LARU) were divided into different cohorts with five mice in each group ($n = 5$). Mice were injected subcutaneously (area at the neck) with 50 µl solution of the tested vaccine formulations: ACNs-lipoj14-KLH, ACNs-lipoj14-KLH-poly (I:C), and physical mixture (ACNs+lipoj14+KLH) which contained 30 µg immunogen on day 0, followed by booster doses on Day 21, 31 and 41. The negative control group received normal saline at a total volume of 50 µl. The positive control group was administered with 50 µl lipoJ14 emulsified with CFA and was boosted with 30 µg of lipoJ14 in 50 µl normal saline at similar immunization interval.

2.8. Collection of blood samples and organ of interest

A 10 ul blood was collected from each mouse, one day prior to immunization via tail bleed, while the final blood samples on Day 50 were collected by cardiac puncture. Blood was left to clot at 37 °C for 1 h and centrifuged for 10 min at 3000 rpm to separate the serum. Serum samples were stored at −80 °C until further analysis. Mice were sacrificed, and vital organ including liver, kidney were dissected out and fixed in 4% (v/v) buffered formalin for preservation until further used and spleen were kept at −80 °C until further analysis.

2.9. Determination of antibodies production

Detection of serum IgG, IgG1 and IgG2a antibodies against J14 epitope was performed using an enzyme linked immunosorbent assay (ELISA) as previously reported [23,24]. In short, ELISA plates were coated with J14 (10 mg/ml) in ELISA carbonate coating buffer overnight at 4 °C and blocked with 150 µl/well of (3% BSA in PBS with 0.05% Tween-20) for 90 min at 37 °C. Serial dilutions of collected sera were prepared using reagent diluent (0.1% BSA in PBS, with 0.05% Tween-20) starting at 1:100 concentration followed by 1:2 dilutions. Absorbance values were read at 450 nm in a microplate reader

after the addition of secondary antibody (antimouse-IgG conjugated to horseradish peroxidase mixture with hydrogen peroxide and tetramethylbenzidine). The antibody titre was identified as the lowest dilution that give absorbance of more than 3 standard deviations above the mean absorbance of control wells (contains normal mouse serum). Statistical analysis ($P < 0.05$ = statistical significance) was performed with one-way ANOVA followed by Turkey post hoc test. For the IgG subtype detection, mice sera from each group were pooled together and ELISA analysis for the tested antibody isotypes (horse radish peroxidase-conjugated sheep anti-mouse IgG1 and IgG2a) was performed using similar protocol in duplicates for each group.

2.10. *Cytokine profiling*

Cytokines secretion from the immunized mice were quantified using a PrimePLex Proteomics Immunoasssay (MULTIPLEX) according to the manufacturer's protocol. Analytes included in the MULTIPLEX kit were IFN-γ, IL-2 and IL-4. Initially, the collected spleens were immersed with RIPA buffer followed by crushing through sonicator (Model MSX-Q125220, Qsonica,USA) to obtain a single-cell suspension. Then the lysates of each group were subjected to centrifugation at 14 000 rpm for 10 min at 4 °C. The culture supernatants were aliquot and transferred into 96 round bottom-well plate. The cytokines expression was quantified based on mean fluorescence intensities based on curve plotting provided by the manufacturer. All samples were run in triplicate.

2.11. *Indirect bactericidal assay*

The mouse sera samples from immunized mice were analyzed for their ability to induce opsonization against different GAS strains. The tested GAS strains include a clinical isolate streptococcus pyogenes (obtained from Hospital Cancelor Tunku Mukhriz of UKM) and streptococcus pyogenes ATCC 19,615. The bacterium was streaked on a Todd–Hewitt broth supplemented with 5% yeast extract agar plate, and incubated at 37 °C for 24 h. Then, a single colony from the bacterium was transferred to 5 ml Todd-Hewitt broth supplemented with 5% yeast extract. The suspension was grown overnight at 37 °C to give approximately 4.6×10^6 colony forming units (CFU)/ml. The culture was serially diluted to 10^2 in PBS and an aliquot (10 µl) was mixed with freshly heat-inactivated sera (10 µl) and horse blood (80 µl). The sera were inactivated by heating in water bath at 50 °C for 30 min. Inoculum of bacteria were incubated together with the presence of sera inside a 96-well plate at 37 °C for 3 h. An aliquot (10 µl) was withdrawn from the culture material and plated on Todd-Hewitt agar plates (supplemented with 5% yeast extract and 5% horse blood) to analyze the bacteria survival. Plates were incubated at 37 °C for 24 h and colonies were counted to CFU. The assay was performed in triplicate from three independent cultures. Opsonic activity of the antibodies (anti-peptide) sera (percentage reduction in mean CFU) was calculated by using the following formula: (1 - [mean CFU in the presence of immunized sera]/[*mean CFU in the presence of normal saline administered mice*]) × 100.

2.12. *In vitro cytotoxicity assay*

Cytotoxicity assay on human embryonic kidney cells (HEK293) was performed as described elsewhere [21]. HEK293 cells were cultured at 37 °C with 5% CO_2 in EMEM (supplemented with 10% FBS and 1% penicillin/streptomycin). 200 µl of each cell (with cell density of 1.0×10^4 cells/well) was seeded into a clear 96 well-plate and incubated in similar aforementioned conditions for 24 h. Formulated vaccines were prepared at concentration ranging from 0.03125 to 1.0 mg/ml and were serially diluted using EMEM with 1% acetic acid. Previous media were removed and 200 µl of each dilution weas added into each well containing the attached cells in triplicate and incubated at 37 °C with 5% CO_2 for 24 h. Then, 20 µl MTT dye solution (5 mg/ml) was added into each well and incubated for 4 h at 37 °C. The MTT solution media was removed and replaced with 100 µl DMSO to solubilize the formed formazan crystal. Untreated cells were used as negative control and DMSO alone was used as a blank. The absorbance was read at 570 nm using NanoQuant infinite M200 PRO spectrophotometric microplate reader (Tecan, Switzerland). The cell viability data was determined by using the following formula:

$$\text{Cell viability (\%)} = (\text{AbsCompound} - \text{AbsBlank}/\text{AbsNegative} - \text{AbsBlank}) \times 100\%$$

2.13. *In vivo toxicity evaluation (physical observation and histopathological examination)*

Experimental mice were closely monitored throughout the immunization period for signs of toxicity in terms of behavioural changes and mortality. Body weight was recorded at every pre-determined interval time frame. The collected vital organs (liver and kidneys) were evaluated for histopathological examination. Briefly, the tissues were dehydrated with ethyl alcohol, followed by treatment with ethyl salicylate. Next, the tissue was embedded in a paraffin wax block. Then the sample were cut at the 2-µm thickness and mounted on a microscopic slide. The sections were stained with hematoxylin and eosin (H&E) for examination under microscope.

3. Results and discussion

3.1. *Preparation and characterizations of nanoparticle-based peptide vaccines*

The chitosan backbone was functionalized with arginine and oleic acid to produce the amphiphilic chitosan derivative. Both arginine and oleic acid were grafted to the reactive amino groups present in chitosan by amidation through the EDC-mediated reaction. The conjugation was confirmed by IR spectra as shown in (Fig. 2). The commonly observed C = O stretch of the CH2, amide I and -OH bands of chitosan was observed in the spectra of chitosan at 1385 cm^{-1},1643 cm^{-1} and 3410 cm^{-1} respectively [25,26]. The existence of additional peak at ~1567 cm^1 (comparable peak at both chitosan-

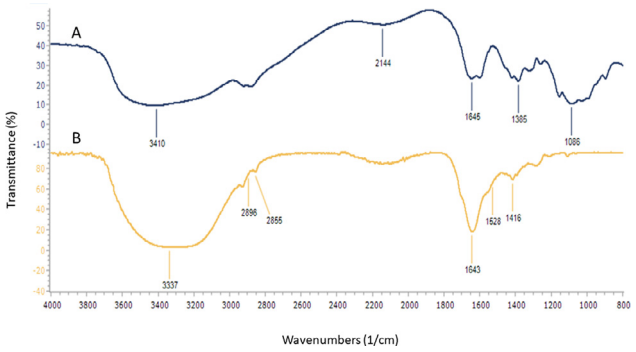

Fig. 2 – FTIR spectrum of (A) chitosan, (B) chitosan-arginine (C) chitosan-oleic acid and (D) amphiphilic chitosan.

arginine and chitosan oleic acid spectra) in the spectra of the amphiphilic chitosan derivative in comparison to native chitosan most likely indicated the appearance characteristic of the newly formed amide II bond, which demonstrated the conjugation of oleic acid/arginine to the chitosan backbone. Comparing the noticeable band at 1557 cm^{-1} of amphiphilic chitosan derivative with those of chitosan and chitosan-arginine (observed peak at 1549 $cm^{-1)}$, there was a visible additional peak that might be corresponded to the guanidine group of arginine. Likewise, the presence of new peaks at 2852–2927 cm^{-1} in the FTIR spectra of chitosan-oleic acid and amphiphilic chitosan in comparison to chitosan alone was attributed to the addition of a long aliphatic chain of oleic acid [25,27]. This result demonstrated that some proportion of the amino groups of chitosan was substituted with oleic acid. Altogether, the characteristic features of chitosan and amphiphilic-modified chitosan spectrum in this study were comparable to our previous report [21]. The structural characteristic of the synthesized amphiphilic chitosan was further verified by using ^{1}H NMR (Fig. S1). The verification was done by determined the overlapping ^{1}H NMR spectra of the synthesized amphiphilic chitosan with the starting materials (chitosan, oleic acid and arginine). The presence of peaks at the region of 2.88–3.30 ppm represents the glucose backbone of chitosan. By comparison of the ^{1}H NMR spectra of the amphiphilic chitosan with pure oleic acid, one can clearly observed the presence of peaks within the region 5.32–5.43 ppm which corresponded to the alkene functional group after the ninth carbon from its carboxyl end, which was comparable to the chemical shift as in pure oleic acid. The conjugation of arginine and oleic acid through the new amide bond formation was observed in the region 7.20–8.02 ppm, indicating the generation of amphiphilic chitosan derivative. Additionally, the recorded ^{1}H NMR of the synthesized amphiphilic chitosan derivative demonstrated comparable characteristic peaks of similar compound to the previous report [21]. The possible reason for non-typical peaks observed was probably due to the effect of depolymerization as reported in previous findings [28].

In our multi-adjuvanted vaccine formulation (ACNs-lipoJ14-KLH) (Fig. 1), the newly synthesized chitosan derivative with enhanced amphiphilic properties was used as the nanoparticle core (ACNs), encapsulated with KLH and intercalated with lipoJ14 within the lipidic portion of ACNs. Additional vaccine formulation with similar compositions supplemented with poly (I:C), abbreviated as ACNs-lipoJ14-KLH-(poly I:C) was also prepared. The encapsulation of KLH, intercalation of lipoJ14 and nanoparticles assembly of the amphiphilic chitosan derivative was facilitated by TPP as a cross-linker. In ACNs-lipoJ14-KLH-(poly I:C) formulation, the functionalization of the ACNs surface with poly (I:C) was mediated by electrostatic interaction.

The physicochemical properties, such as hydrodynamic particle size, size distribution and zeta potential (electric charge on the nanoparticle's surface) of both nanoparticle vaccine formulations were presented in Table 1. Both formulations exhibited particle size within the range of 223–240 nm. However, ACNs-lipoJ14-KLH-(poly I:C) exhibited slightly smaller size (decreased by ~10 nm) nanoparticles in comparison to ACNs-lipoJ14-KLH. This might be due to the positively charged surface of ACNs was compressed by the electrostatic force of the negatively charged poly (I:C). ACNs-lipoJ14-KLH possessed a net positive charge on its surface with a zeta potential value of +27 mV while ACNs-lipoJ14-KLH-(poly I:C) showed a negative zeta potential value (−31 mV). The end-point of successful poly (I:C) coating was determined when the concentration used produced reverted-charged particles (when a large negative zeta potential was observed as shown in Table 1). Although vaccine formulation with additional poly (I:C) coating showed an increase in PDI value, it was still within the acceptable range for a uniform particles size distribution. TEM images revealed that the formulated vaccines exhibited spherical-shaped particles with comparable size dimension as determined by DLS measurement (Fig. 3). A lightly shaded area was observed in ACNs-lipoJ14-KLH-(poly I:C) that represent a successful coating with poly (I:C) (Fig. 3D). Additionally, both vaccine formulations exhibited a high percentage (> 86%) of lipoJ14 encapsulation efficiency and achieved approximately ~53% encapsulation efficiency of KLH. The high loading efficiency of lipoJ14 obtained in both formulations indicating that our strategy in introducing lipid moiety to J14 enhanced its adsorption to the lipidic portion of ACNs via hydrophobic interaction.

3.2. *In vitro uptake study by antigen-presenting cells*

In any vaccine development, it is essential that the formulated vaccine can induce molecular uptakes by the APCs, particularly DCs and macrophages, for further activation and immunological processing by the immune cells [16]. To facilitate recognition by APCs, our nanoparticles vaccines were designed to exhibit size within the nano-range, a comparable dimension to bacteria and viruses. Vaccine formulation in the form of a physical mixture (ACNs + lipoJ14 + KLH) was also included in this study. Generally, the nanoparticles vaccine formulations were preferentially taken up by dendritic cells compared to macrophages (Fig. 4). This is in line with many studies which indicated that smaller particle size (particle diameter less than 500 nm) was ideal for DCs uptake [16,29]. For macrophages, only ACNs-lipoJ14-KLH was taken up at a significant percentage.

Table 1 – Physicochemical properties and encapsulation efficiency of the formulated nanoparticles vaccines.

Nanoparticle formulations	PS (nm)	ZP (mV)	PDI	EE lipoJ14 (%)	EEKLH (%)
ACNs-lipoJ14-KLH	240 ± 2.8	+27 ± 0.6	0.1	96 ± 0.02	55 ± 0.27
ACNs-lipoJ14-KLH-(poly I:C)	223 ± 3.7	−31 ± 0.4	0.3	86 ± 0.09	51 ± 0.10

PS – Particle Size; ZP – Zeta Potential; PDI– Polydispersity Index; EE –Encapsulation Efficiency.

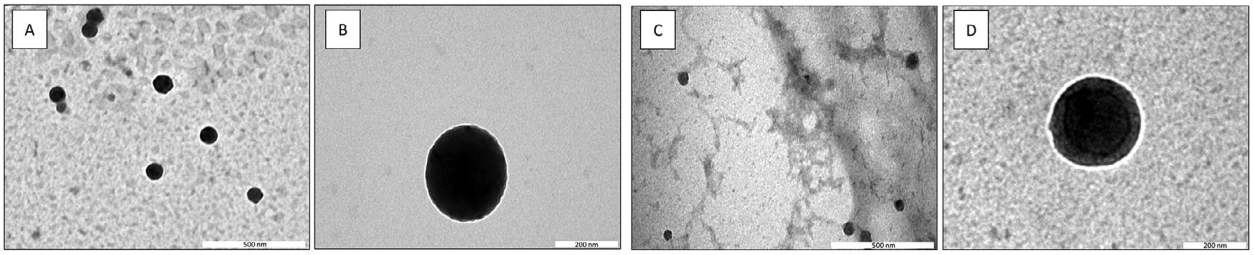

Fig. 3 – Morphology of (A) ACNs-lipoJ14-KLH nanoparticles, (B) single ACNs-lipoJ14-KLH particle, (C) ACNs-lipoJ14-KLH-(poly I:C) nanoparticles and (D) single ACNs-lipoJ14-KLH-(poly I:C) particle as visualized by TEM.

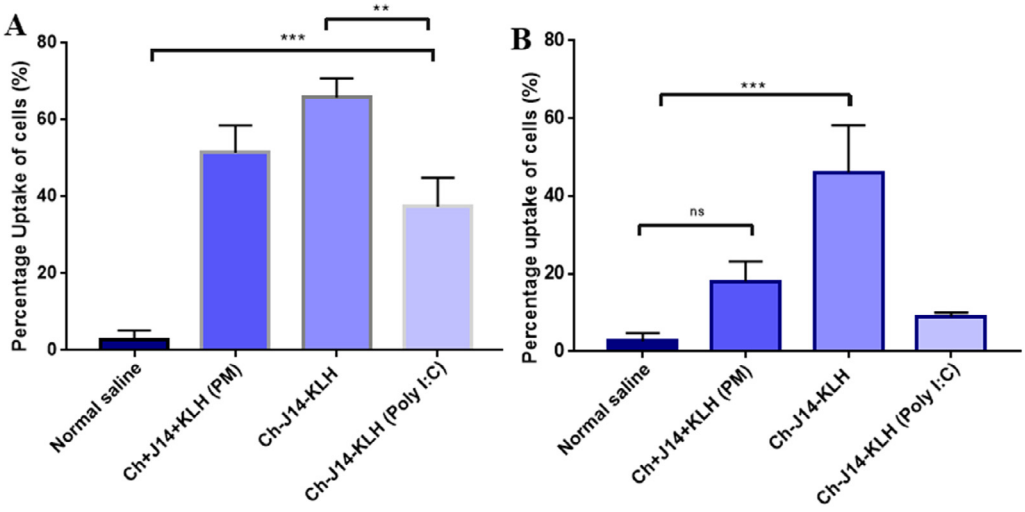

Fig. 4 – Uptake analysis of the tested vaccine formulations by mouse splenocytes-derived dendritic cells (A) and macrophages (B). Statistical analysis performed by one-way ANOVA followed by the Tukey Post-Hoc test (ns, $P > 0.05$; *$P < 0.05$; **$P < 0.01$; ***$P < 0.001$; ****$P < 0.0001$).

Among the tested vaccine formulations, the ACNs-lipoJ14-KLH exhibited the highest uptake by the studied APCs, followed by its physical mixture counterpart formulation (ACNs+J14+KLH) and nanoparticles formulation with an additional layer of poly (I:C). The uptake of ACNs-lipoJ14-KLH by both DCs and macrophages was significantly higher than ACNs-lipoJ14-KLH-(poly I:C). We postulated that the negatively charged surface of ACNs-lipoJ14-KLH-(poly I:C) exerted a repulsive force with the negatively-charged APC's cell membrane. A higher uptake of nanoparticle formulation (ACNs-lipoJ14-KLH) by DCs than its physical mixture counterparts was observed, even though it was not statistically significant. This data shown that by associating the vaccine antigen with a particulate delivery system enhanced its uptake by the APCs compared to when the antigen was formulated by a simple physical mixture. However, it is important to note that higher uptake by APCs may not necessarily contribute to a greater immune response induction [3]. Thus, it is necessary to evaluate the efficacy of the vaccine formulations *in vivo*.

3.3. *Immunogenicity of the vaccine formulations* in vivo

The immunogenicity of the nanoparticle vaccine formulations was assessed in Balb/c mice. Groups of five mice were immunized with normal saline as (negative control), lipoJ14 emulsified in CFA (positive control), ACNs-lipoJ14-KLH-(poly I:C), ACNs-lipoJ14-KLH and a physical mixture formulation (ACNs + lipoJ14 + KLH). Significantly, elevated J14-specific IgG titers were observed for all tested formulations containing

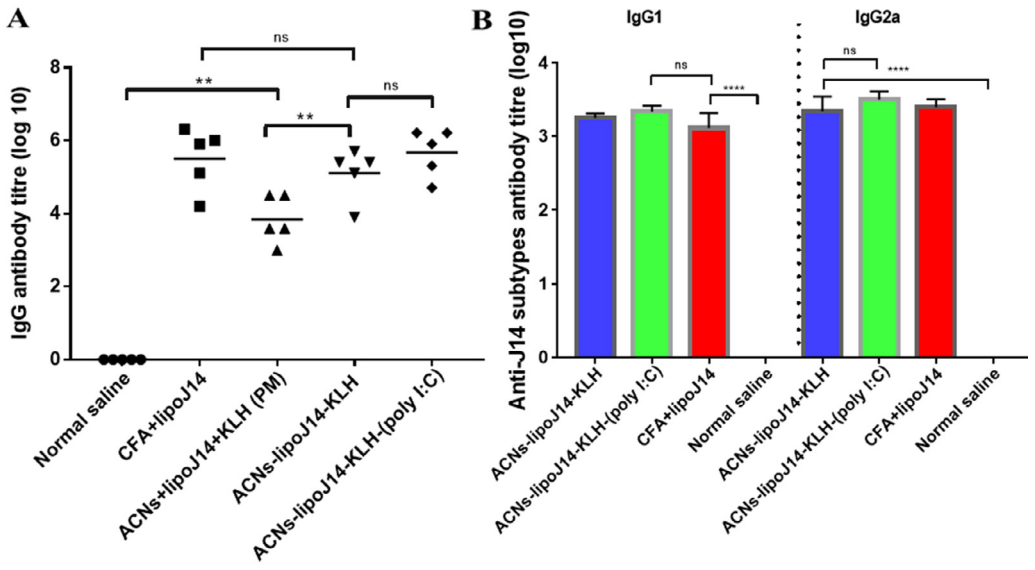

Fig. 5 – J14-specific antibody productions at the final bleed after prime-boost vaccination (A) J14-specific IgG antibody titters in collected serum of individual BALB/c mice ($n = 5$/group). The mean J14-specific IgG titers are represented as a bar. (B) Titers of J14-specific serum IgG1 and IgG2a from pooled sera of each group. Statistical analysis was performed using one-way ANOVA followed by Turkey Post-Hoc test between groups as indicated (ns: $p > 0.05$; *P < 0.05; **P <0.01; ***P < 0.001; ****P < 0.0001).

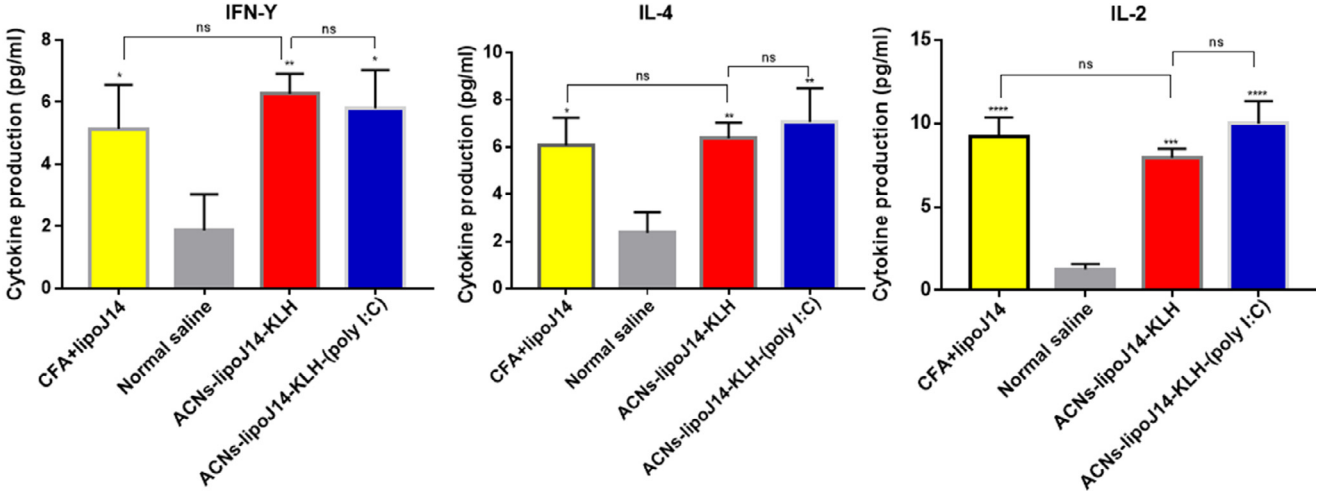

Fig. 6 – Level of splenocyte cytokines response prior to immunization. Bars represent mean concentrations ± SD. Statistical analysis of cytokines concentrations secreted form the test groups was performed using one-way ANOVA followed by Turkey's multiple comparisons between groups as indicated (NS: P > 0.05; *P < 0.05; **P <0.01; ***P < 0.001; ****P < 0.0001).

lipoJ14. As shown in Fig. 5A, both ACNs-lipoJ14-KLH and ACNs-lipoJ14-KLH-(poly I:C) induced comparable J14-specific systemic IgG titers to the mice group that was immunized with positive control used in this study (lipoJ14-CFA emulsion). CFA is a potent adjuvant and regarded as the "gold standard" to serve as a positive control in peptide vaccine development [11,30]. However, due to its toxicity, CFA is not recommended to be used in a clinical setting. Although ACNs-lipoJ14-KLH-(poly I:C) elicited higher IgG titers than ACNs-lipoJ14-KLH, the difference was not statistically significant. Notably, with similar vaccine compositions, the nanoparticles formulation (ACNs-lipoJ14-KLH) induced significantly higher IgG antibody titters ($P < 0.05$) than the physical mixtures (ACNs + lipoJ14 +KLH). This data showed that encapsulation of subunit vaccine into particulate vaccine delivery system facilitated greater recognition by immune cells for efficient modulation of the immune response.

Pooled serum from mice immunized with ACNs-lipoJ14-KLH and ACNs-lipoJ14-KLH-(poly I:C) formulations were

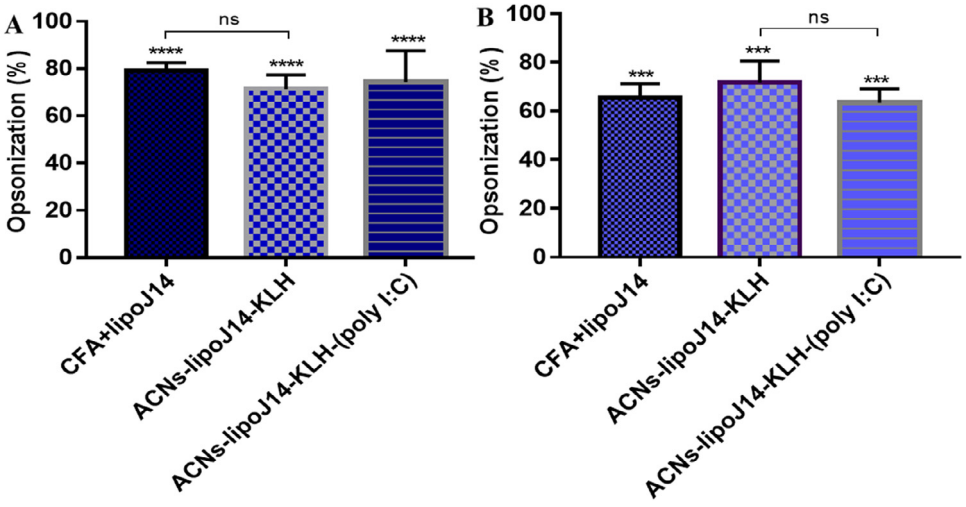

Fig. 7 – Average percentage opsonization of serum against ATCC 19,615 (A) and clinically isolated (B) group A streptococcus strains in Balb/c mice ($n = 3$). Statistical analysis was performed using one-way ANOVA followed by Turkey Post-Hoc test compared with normal saline-administered mice as indicated (ns, $P > 0.05$; *$P < 0.05$; **$P < 0.01$; ***$P < 0.001$).

further evaluated for IgG1 and IgG2a antibody isotypes production. Both formulations induced comparable IgG1 and IgG2a titers to CFA-adjuvanted lipoJ14 (Fig. 5B). CFA is known to be effective in inducing both humoral responses (Th2) and cell-mediating immunity (Th1), with slightly biased towards Th1 polarization [31,32]. It can be deduced that ACNs-lipoJ14-KLH and ACNs-lipoJ14-KLH (poly I:C) polarized a balanced Th1 and Th2 immune response as characterized by the level of IgG1 and IgG2a titers, respectively.

We further examined the release of cytokines by splenocytes cells from mice immunized with both nanoparticle vaccine formulations to establish the involvement of Th cell-derived cytokines in the adjuvanting activity of our vaccine carrier. The levels of cytokines present in the culture supernatant of splenocytes from each tested group are shown in Fig. 6. A panel of three cytokines, IFN-γ and IL-2 that typically associated with Th1 response and 1L-4 that corresponds to Th2 polarization were quantified. Generally, splenocytes from the immunized groups secreted significant levels of the tested cytokines in comparison to the negative control group. Higher secretion of IL-4 was observed with ACNs-lipoJ14-KLH-(poly I:C) compared to ACNs-lipoJ14-KLH and positive control group. ACNs-lipoJ14-KLH elicited higher levels of IFN-γ, but lower levels of IL-2 compared to similar formulation with additional poly (I:C) coating and lipoJ14 adjuvanted with CFA. However, it is important to note that the different levels of cytokines secretion between ACNs-lipoJ14-KLH-(poly I:C), ACNs-lipoJ14-KLH and lipoJ14-CFA emulsion were not statistically significant. Taken together, we showed that our vaccine formulation strategy does not induce a specific Th subset, but rather potentiated both Th1 and Th2 immune response, regardless of the presence of poly (I:C) coating. This is highly advantageous as a recent study has reported that both cellular and humoral immunity are predominant following natural exposure to GAS in human [33].

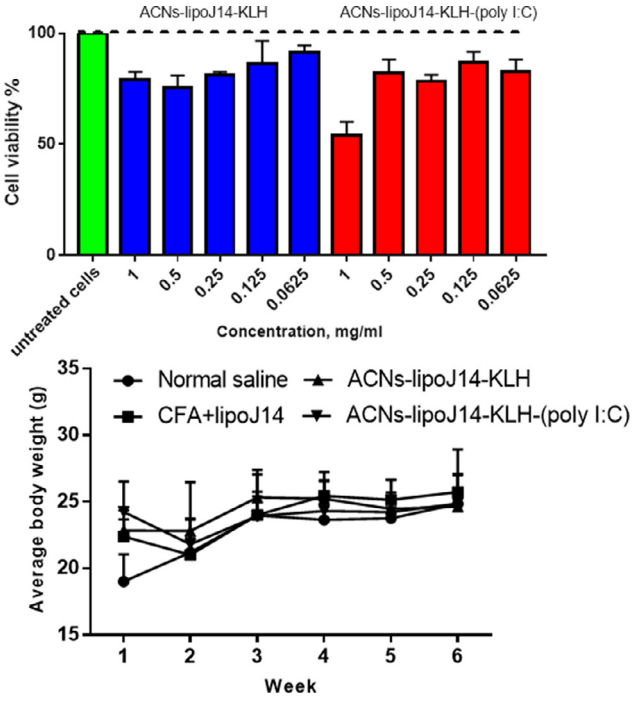

Fig. 8 – Toxicity evaluations of formulated vaccine candidates (A) Cell viability assay on HEK293 cell line with various concentrations, the data is reported as mean ± SD, $n = 3$. (B) Average body weight changes of mice before and during the immunization schedule.

3.4. *Opsonizing antibodies against GAS*

Protection against GAS infections is highly associated with opsonizing antibodies production. The opsonizing antibodies are highly associated with immune protection against GAS

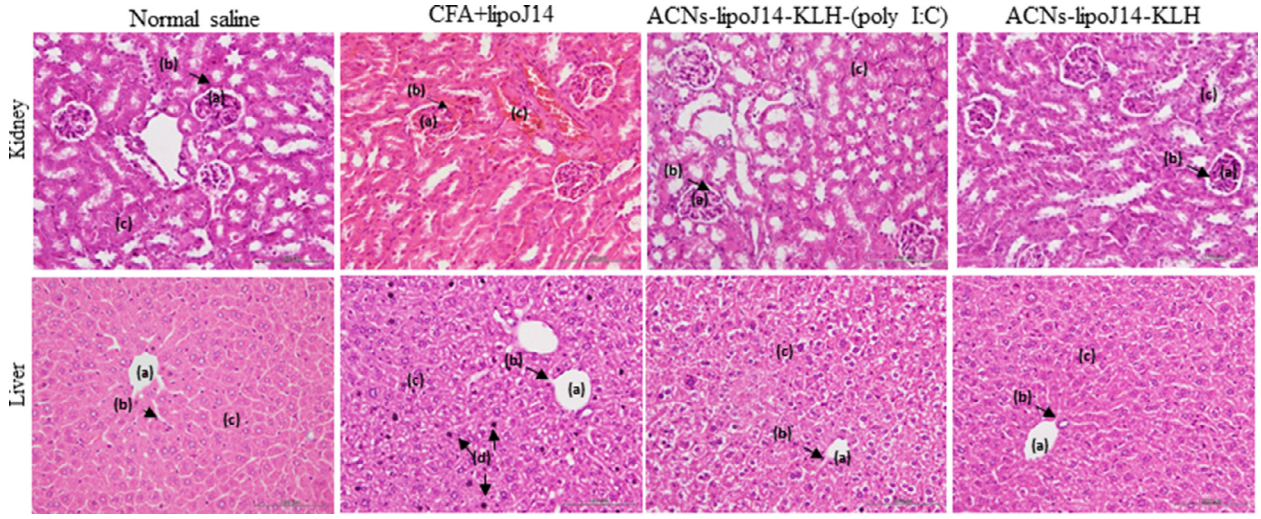

Fig. 9 – Photomicrographs section (H & E stains) from immunized mice with various vaccine candidates. Kidney:(a) renal corpuscle (b) capsular space and (c) convoluted tubule. Liver: (a) central vein (b) sinusoid (c) hepatocytes and (d) Kupffer cells.

infections [34,35]. In order to determine the opsonization capabilities of the antibodies produced, sera from immunized mice groups with nanoparticles vaccine formulations and positive control were tested against ATCC and clinically isolated strains of GAS. Antibodies produced in sera derived from both nanoparticle vaccines ACNs-lipoJ14-KLH-(poly I:C) and ACNs-lipoJ14-KLH induced high opsonic activity (ranged within 65% to 80%) against the tested GAS strains (Fig. 7) The opsonization activities of the antibodies produced from mice immunized with of our formulations are statistically comparable to the mice group administered with CFA adjuvanted vaccine antigen. The overall immunogenicity evaluations demonstrated that our amphiphilic modified chitosan nanoparticles, supplemented with KLH and either with or without additional coating with poly (I:C) raised potent J14-opsonizing antibodies driven by Th1 and Th2 immunity. This data demonstrated that the inclusion of poly (I:C) in the vaccine formulation may not be necessary in inducing the significant immune responses.

3.5. *Toxicity evaluations*

Safety is one of the mandatory criteria for successful vaccine development. The toxicity evaluations of the formulated nanoparticles vaccines were performed *in vitro* and *in vivo*. For cytotoxicity evaluations, various concentrations of ACNs-lipoJ14-KLH-(poly I:C) and ACNs-lipoJ14-KLH were tested against HEK293 (embryonic human kidney cells) by using MTT assay. The viability of the HEK293 cells upon treatment with our vaccine formulations are depicted in Fig. 8A. Generally, percentages of cell viability exceeding 80% is considered as non-cytotoxicity [21]. The MTT assay data revealed that the formulated nanoparticles vaccines were not toxic to the HEK293 cells up until 0.5 mg/ml. However, at 1 mg/ml, ACNs-lipoJ14-KLH-(poly I:C) showed a reduction in cell viability (~50%). Considering the low dose of vaccination, the extremely high concentration (>200 fold higher than vaccination dose) of the vaccine that caused ~50% cell viability could be negligible. The reactogenicity of mice towards the nanovaccine candidates were accessed upon immunization by monitoring illness, death and weight loss. No death or symptoms of adverse reactions were observed throughout the immunization period in mice. Average reduction in body weight was observed for groups of mice upon receiving their first dose of vaccines (Fig. 8B). No weight loss was observed for unvaccinated group of mice at similar time frame. Nevertheless, the average weight of all the immunized groups of mice showed an increasing trend and was comparable to unvaccinated group after the administration of three booster doses.

On Day 50, mice were sacrificed and major organs such as liver and kidney were isolated for histopathological assessment. As shown in Fig. 9, no significant changes were observed between the unvaccinated mice and those vaccinated with ACNs-lipoJ14-KLH-(poly I:C) and ACNs-lipoJ14-KLH in the photomicrographs of the examined organs. In contrast, organs derived from the positive control group, which was adjuvanted with CFA demonstrated histopathological lesions in liver and kidney. Additionally, the presence of kupffer cells in the liver tissue of the mice group vaccinated with CFA indicating a response towards liver injury [36]. The kidney tissue in the CFA-adjuvanted mice group showed interstitials inflammatory infiltration and cast at the glomerulus and convoluted tubules [37].

4. Conclusion

In the present work, amphiphilic chitosan derivative (functionalized with arginine and oleic acid) was successfully prepared and used as a core in the nanoparticle vaccine formulations containing a carrier protein KLH and lipoJ14 as an antigen. The cellular uptake studies showed that the formulated vaccines possessed physicochemical properties, such as nano-range particles size that facilitated their efficient uptake by the APCs, particularly DCs. Our immunological

assessment in mice showed that the nanoparticle vaccine formulations, even without additional coating with poly (I:C), managed to induce significant immune responses as characterized by antibodies productions, cytokines secretions and its relatively high opsonic activity. These findings suggested that the amphiphilic chitosan nanoparticles modulated a potent adjuvanting activity on the specific cellular and humoral immune response, without the need for any additional TLR agonist, such as poly (I:C). Furthermore, we also highlighted the importance of co-delivery of peptide antigen alongside immunostimulant materials in single nanoparticulate form to augment an efficacious immune response. The ability of our amphiphilic chitosan-based vaccine delivery platform in generating a balanced Th1/Th2 would create a new paradigm in the search for an effective carrier for peptide vaccine against GAS.

Conflicts of interest

The authors report no conflicts of interest. The authors alone are responsible for the content and writing of this article.

Acknowledgements

This research was supported financially by Universiti Kebangsaan Malaysia (UKM), Malaysia [DCP-2017–003/2].

Supplementary materials

Supplementary material associated with this article can be found, in the online version, at doi:10.1016/j.ajps.2022.04.002.

REFERENCES

[1] World Health Organization. The current evidence for the burden of group a streptococcal a. diseases. Geneva, Switzerland: WHO; 2005. p. 1–52.
[2] Minodier P, Laporte R, Miramont S. Epidemiology of Streptococcus pyogenes infections in developing countries. Arch Pediatr 2014:69–72.
[3] Marasini N, Giddam AK, Khalil ZG, et al. Double adjuvanting strategy for peptide-based vaccines: trimethyl chitosan nanoparticles for lipopeptide delivery. Nanomed (Lond) 2016;11(24):3223–35.
[4] Passàli D, Lauriello M, Passàli GC, Passàli FM, Bellussi L. Group A streptococcus and its antibiotic resistance. Acta Otorhinolaryngol Ital 2007;27(1):27–32.
[5] Castro SA, Dorfmueller HC. A brief review on group A streptococcus pathogenesis and vaccine development. R Soc Open Sci 2021;8(3):201991.
[6] Dale JB, Batzloff MR, Cleary PP, Courtney HS, Good MF, Grandi G, et al. Current approaches to group A streptococcal vaccine development Streptococcus pyogenes: basic biology to clinical manifestations. Ferretti JJ, Stevens DL, Fischetti VA, editors. editors. Oklahoma City (OK): University of Oklahoma Health Sciences Center; 2016.
[7] Giffard PM, Tong S, Holt DC, Ralph AP, Currie BJ. Concerns for efficacy of a 30-valent M-protein-based Streptococcus pyogenes vaccine in regions with high rates of rheumatic heart disease. PLoS Negl Trop Dis 2019;13(7):e0007511.
[8] Mertens NMJ, et al. Molecular analysis of cross-reactive anti-myosin/anti-streptococcal mouse monoclonal antibodies. Mol Immunol 2000;37(15):901–13.
[9] Pruksakorn S, Currie B, Brandt E, Phornphutkul C, Hunsakunachai S, Manmontri A, Good MF. Identification of T cell autoepitopes that cross-react with the C-terminal segment of the M protein of group A streptococci. Int Immunol 1994;6(8):1235–44.
[10] Hayman WA, Brandt ER, Relf WA, Cooper J, Saul A, Good MF. Mapping the minimal murine T cell and B cell epitopes within a peptide vaccine candidate from the conserved region of the M protein of group A streptococcus. Int Immunol 1997;9(11):1723–33.
[11] Azmi F, Ahmad Fuaad AA, Skwarczynski M, Toth I. Recent progress in adjuvant discovery for peptide-based subunit vaccines. Hum Vaccin Immunother 2014:778–96.
[12] Azmi F. Revolutionary approach in the application of toll-like receptor agonist in Nanoparticles formulation for peptide-based subunit vaccine. Vaccin Res Open J 2018;8(1):Se1–3 SE.
[13] Skwarczynski M, Toth I. Peptide-based synthetic vaccines. Chem Sci 2016;7(2):842–54.
[14] Malik A, Gupta M, Gupta V, Gogoi H, Bhatnagar R. Novel application of trimethyl chitosan as an adjuvant in vaccine delivery. Int J Nanomedicine 2018;13:7959–70.
[15] Li P, Wang F. Polysaccharides: candidates of promising vaccine adjuvants. Drug Discov Ther 2015;9(2):88–93.
[16] Marasini N, Giddam AK, Ghaffar KA, Batzloff MR, Good MF, Skwarczynski M, et al. Multilayer engineered nanoliposomes as a novel tool for oral delivery of lipopeptide-based vaccines against group A Streptococcus. Nanomedicine 2016;11(10):1223–36.
[17] Sales-Campos H, Souza PR, Peghini BC, da Silva JS, Cardoso CR. An overview of the modulatory effects of oleic acid in health and disease. Mini Rev Med Chem 2013;13(2):201–10.
[18] Nguyen MT, Götz F. Lipoproteins of gram-positive bacteria: key players in the immune response and virulence. Microbiol Mol Biol Rev 2016;80(3):891–903.
[19] Moyle PM, Dai W, Zhang Y, Batzloff MR, Good MF, Toth I. Site-specific incorporation of three toll-like receptor 2 targeting adjuvants into semisynthetic, molecularly defined nanoparticles: application to Group A Streptococcal vaccines. Bioconjug Chem 2014;25(5):965–78.
[20] Zaman M, Abdel-Aal ABM, Fujita Y, Ziora ZM, Batzloff MR, Good MF, et al. Structure–activity relationship for the development of a self-adjuvanting mucosally active lipopeptide vaccine against Streptococcus pyogenes. J Med Chem 2012:8515–23.
[21] Ahmad N, Wee CE, Wai LK, Zin NM, Azmi F. Biomimetic amphiphilic chitosan nanoparticles: synthesis, characterization and antimicrobial activity. Carbohydr Polym 2021;254:117299.
[22] Ghaffar KA, Marasini N, Giddam AK, Batzloff MR, Good MF, Skwarczynski M, et al. Liposome-based intranasal delivery of lipopeptide vaccine candidates against group A streptococcus. Acta Biomater 2016;41:161–8.
[23] Azmi F, Ahmad Fuaad AA, Giddam AK, Batzloff MR, Good MF, Skwarczynski M, et al. Self-adjuvanting vaccine against group A streptococcus: application of fibrillized peptide and immunostimulatory lipid as adjuvant. Bioorg Med Chem 2014;22(22):6401–8.
[24] Chen XY, Butt AM. Mohd Amin MCI. Molecular evaluation of oral immunogenicity of hepatitis B antigen delivered by hydrogel microparticles. Mol Pharm 2019;16(9):3853–72.
[25] Xiao B, Wan Y, Zhao M, Liu Y, Zhang S. Preparation and characterization of antimicrobial chitosan-N-arginine with

different degrees of substitution. Carbohydr Polym 2011;83(1):144–50.
[26] Bianchera A, Salomi E, Pezzanera M, Ruwet E, Bettini R, Elviri L. Chitosan hydrogels for chondroitin sulphate controlled release: an analytical characterization. J Anal Methods Chem 2014:808703.
[27] Liu WG, Zhang JR, Cao ZQ, Xu FY, Yao KD. A chitosan-arginine conjugate as a novel anticoagulation biomaterial. J Mater Sci Mater Med 2004;15(11):1199–203.
[28] Kumirska J, Weinhold MX, Sauvageau JCM, Th¨oming J, Stepnowski P. Determination of the pattern of acetylation of low-molecular-weight chitosan used in biomedical applications. J Pharm Biomed Anal 2009;50:587–90.
[29] Slütter B, Plapied L, Fievez V, Sande MA, des Rieux A, Schneider YJ, et al. Mechanistic study of the adjuvant effect of biodegradable nanoparticles in mucosal vaccination. J Control Release 2009;138(2):113–21.
[30] Azuar A, Jin W, Mukaida S, Hussein WM, Toth I, Skwarczynski M. Recent advances in the development of peptide vaccines and their delivery systems against group A Streptococcus. Vaccines (Basel) 2019;7(3).
[31] Shibaki A, Katz SI. Induction of skewed Th1/Th2 T-cell differentiation via subcutaneous immunization with Freund's adjuvant. Exp Dermatol 2002;11(2):126–34.
[32] Shenderov K, Barber D, Mayer K, Jankovic D, White S, Caspar P, et al. Inflammasome-dependent IL-1β production is critical for complete Freund's adjuvant-induced helper T cell polarization (136.44). J Immunol 2010;184:136–44.
[33] Mortensen R, Nissen TN, Fredslund S, Rosenkrands I, Christensen JP, Andersen P, Dietrich J. Identifying protective Streptococcus pyogenes vaccine antigens recognized by both B and T cells in human adults and children. Sci Rep 2016;6:22030.
[34] Penfound TA, Chiang EY, Ahmed EA, Dale JB. Protective efficacy of group A streptococcal vaccines containing type-specific and conserved M protein epitopes. Vaccine 2010;28(31):5017–22.
[35] Tsoi SK, Smeesters PR, Frost HR, Licciardi P, Steer AC. Correlates of protection for M protein-based vaccines against group A Streptococcus. J Immunol Res 2015:167089.
[36] Han J, Ulevitch RJ. Limiting inflammatory responses during activation of innate immunity. Nat Immunol 2005;6(12):1198–205.
[37] Rangel M, Martins JC, Garcia AN, Conserva GA, Costa-Neves A, Sant'Anna CL, de Carvalho LR. Analysis of the toxicity and histopathology induced by the oral administration of Pseudanabaena galeata and Geitlerinema splendidum (cyanobacteria) extracts to mice. Mar Drugs 2014;12(1):508–24.